

Mixed Finite Element Discretization for Maxwell Viscoelastic Model of Wave Propagation *

Hao Yuan [†], Xiaoping Xie [‡]

*School of Mathematics, Sichuan University, Chengdu 610064,
China*

Abstract

This paper considers semi-discrete and fully discrete mixed finite element discretizations for Maxwell-model-based problems of wave propagation in 2-dimensional linear viscoelastic solid. A large class of existing mixed conforming finite elements for elasticity are used in the spatial discretization. In the fully discrete scheme, a Crank-Nicolson scheme is adopted for the approximation of the temporal derivatives of displacement and stress. Error estimates of the two schemes, as well as an unconditional stability result for the fully discrete scheme, are derived. Numerical experiments are provided which apply two low order rectangular elements in the spatial discretization.

Keywords: Maxwell viscoelastic model; wave propagation; mixed finite element; semi-discrete; fully discrete; error estimate; stability

1 Introduction

Let $\Omega \subset \mathbb{R}^2$ be a bounded open domain with boundary $\partial\Omega$ and T be a positive constant. Consider the following Maxwell viscoelastic model of wave propagation:

$$\begin{cases} \rho u_{tt} = \mathbf{div} \sigma + f, & (x, t) \in \Omega \times [0, T], \\ \sigma + \sigma_t = \mathbb{C} \varepsilon(u_t), & (x, t) \in \Omega \times [0, T], \\ u = 0, & (x, t) \in \partial\Omega \times [0, T], \\ u(x, 0) = \phi_0(x), u_t(x, 0) = \phi_1(x), \sigma(x, 0) = \psi_0(x), & x \in \Omega. \end{cases} \quad (1.1)$$

Here $u = (u_1, u_2)^T$ is the displacement field, $\sigma = (\sigma_{ij})_{2 \times 2}$ the symmetric stress tensor, $\varepsilon(u) = (\nabla u + (\nabla u)^T)/2$ the strain tensor, and $g_t := \partial g / \partial t$ and $g_{tt} :=$

*This work was supported in part by National Natural Science Foundation of China (11771312).

[†]Email: kobeyuanhao@qq.com

[‡]Corresponding author. Email: xpxie@scu.edu.cn

$\partial^2 g / \partial t^2$ for any function $g(x, t)$. $\rho(x)$ denotes the mass density and \mathbb{C} the elastic module tensor, with

$$0 < \rho_0 \leq \rho \leq \rho_1 < \infty \quad a.e. \quad x \in \Omega, \quad (1.2)$$

$$0 < M_0 \tau : \tau \leq \mathbb{C}^{-1} \tau : \tau \leq M_1 \tau : \tau \quad \forall \text{ symmetric tensor } \tau = (\tau_{ij})_{2 \times 2} \text{ a.e. } x \in \Omega, \quad (1.3)$$

where ρ_0, ρ_1, M_0 and M_1 are four positive constants, and $\sigma : \tau := \sum_{i=1}^2 \sum_{j=1}^2 \sigma_{ij} \tau_{ij}$.

Note that $\mathbb{C}\varepsilon(u_t)$ is of the form

$$\mathbb{C}\varepsilon(u_t) = 2\mu\varepsilon(u_t) + \lambda \operatorname{div} u_t I \quad (1.4)$$

for an isotropic elastic medium, where μ, λ are the Lamé parameters, I the identity matrix, and $\operatorname{tr}(u_t)$ the trace of u_t . $f = (f_1, f_2)$ is the body force, and $\phi_0(x), \phi_1(x), \psi_0(x)$ are initial data.

Numerous materials simultaneously display elastic and viscous kinematic behaviours. Such a feature, called viscoelasticity, can be characterized by using springs, which obey the Hooke's law, and viscous dashpots, which obey the Newton's law. Different combinations of the springs and dashpots lead to various viscoelastic models, e.g. the three classical models of Zener, Voigt and Maxwell. We note that there is a unified framework to describe the general constitutive law of viscoelasticity by using convolution integrals in time with some kernels [8, 11, 29]; however, the integral forms of constitutive laws, compared with the differential forms, bring more difficulties to the design of algorithms due to the numerical convolution integral. We refer the reader to [5, 9, 10, 11, 12, 13, 30, 31] for several monographs on the development and applications of viscoelasticity theory.

The numerical simulation of wave propagation in viscoelastic materials was first discussed by Kosloff et al. in [20, 21], where memory variables were introduced to avoid the convolutional integral in the constitutive relation. Later, finite difference methods were developed in [6, 28, 34] for the model with memory variables. There are considerable research efforts on the finite element discretization in this field. In [18] Janovsky et al. studied the continuous/discontinuous Galerkin finite element discretization and used a numerical quadrature formula to approximate the Volterra time integral term. Ha et al. [14] proposed a nonconforming finite element method for a viscoelastic complex model in the space-frequency domain. Bécache et al. [3] applied a family of mixed finite elements with mass lumping, together with a leap-frog scheme in time discretization, to numerically solve the Zener model, and showed that their scheme is stable under certain CFL condition. In [24, 25, 26], Rivière et al. analyzed discontinuous Galerkin methods with a Crank-Nicolson temporal discrete scheme for quasistatic linear viscoelasticity and linear/nonlinear diffusion viscoelastic models. Rognes and Winther [27] proposed mixed finite element methods for quasistatic Maxwell and Voigt models using weak symmetry, and used a second backward difference scheme in the full discretization. Lee [22] studied mixed finite element methods with weak symmetry for the Zener, Voigt and Maxwell models and adopted the Crank-Nicolson scheme in temporal discretization. Severino and Guillermo [31] gave an overview of numerical methods for problems in viscoelasticity including finite elements, boundary elements, and finite volume formulations. Kimura et al. [19] studied the gradient flow structure of an

extended Maxwell model with a relaxation parameter and proposed a structure-preserving P1/P0 finite element scheme. Recently, Wang and Xie [33] analyzed a hybrid stress finite element method for the Maxwell model and used a second order implicit difference in the fully discrete scheme.

In this paper, we consider semi-discrete and fully discrete mixed finite element discretizations for the Maxwell viscoelasticity model (1.1). It is shown that a large class of existing mixed conforming finite elements for elasticity apply to this model. In the fully discrete scheme, the Crank-Nicolson scheme is used to approximate the temporal derivatives of velocity and stress variables.

The rest of this paper is arranged as follows. Section 2 introduces notations and weak formulations. Section 3 gives a general mixed conforming finite element framework and carries out the error estimation of the semi-discrete scheme. Section 4 presents the fully discrete scheme and derives stability and error estimates. Finally, numerical examples are provided in Section 5 to verify the theory results when using two low order rectangular elements in the spatial discretization.

2 Weak formulations

We first introduce some notations. For any nonnegative integer r , denote by $H^r(\Omega)$ and $H_0^r(\Omega)$ the standard Sobolev spaces with norm $\|\cdot\|_r$ and semi-norm $|\cdot|_r$. In particular, $H^0(\Omega) = L^2(\Omega)$ is the space of square integrable functions. We adopt the convention that an underline (or double underlines) corresponds to a vector-valued (or tensor-valued) space.

For any vector-valued (or tensor-valued) space X , defined on Ω , with norm $\|\cdot\|_X$, denote

$$L^p([0, T]; X) := \{w : [0, T] \rightarrow X; \|w\|_{L^p(X)} < \infty\},$$

where

$$\|w\|_{L^p(X)} := \begin{cases} (\int_0^T \|w(t)\|_X^p)^{1/p} & \text{if } 1 \leq p < \infty, \\ \text{esssup}_{0 \leq t \leq T} \|w(t)\|_X & \text{if } p = \infty, \end{cases}$$

and $w(t)$ abbreviates $w(x, t)$. For integer $r \geq 0$, the space $C^r([0, T]; X)$ can be defined similarly. In the forthcoming analysis, X may be taken as $\underline{L}^2(\Omega)$, $\underline{H}^r(\Omega)$ and

$$\underline{\underline{H}}(\mathbf{div}, \Omega, S) := \{\tau = (\tau_{ij})_{2 \times 2} \in \underline{\underline{L}}^2(\Omega) \mid \tau_{ij} = \tau_{ji}, \mathbf{div} \tau \in \underline{L}^2(\Omega)\}.$$

For convenience, we use the notation $a \lesssim b$ to denote that there exists a generic positive constant C , independent of the spatial and temporal mesh parameters, h and Δt , such that $a \leq Cb$.

We also need two Gronwall's inequalities [32]:

Continuous Gronwall's inequality. Let $\phi(\cdot)$ be such that

$$\phi_t(t) \leq \rho\phi(t) + \eta(t) \quad \text{for } 0 \leq t \leq T,$$

where $\rho \geq 0$ is a constant and $\eta(\cdot) \geq 0, \eta \in L^1([0, T])$. Then it holds

$$\phi(t) \leq e^{\rho T}(\phi(0) + \int_0^T \eta(s)ds), \quad \forall t \in [0, T]. \quad (2.1)$$

Discrete Gronwall's inequality. Let $g_0 \geq 0$ and two nonnegative sequences $(k_n)_{n \geq 0}$, $(p_n)_{n \geq 0}$ be given. Suppose that the sequence $(\phi_n)_{n \geq 0}$ satisfies

$$\begin{cases} \phi_0 \leq g_0, \\ \phi_n \leq g_0 + \sum_{s=0}^{n-1} p_s + \sum_{s=0}^{n-1} k_s \phi_s, \end{cases} \quad \forall n \geq 1. \quad (2.2)$$

Then it holds

$$\phi_n \leq (g_0 + \sum_{s=0}^{n-1} p_s) \exp\left(\sum_{s=0}^{n-1} k_s\right), \quad \forall n \geq 1. \quad (2.3)$$

We are now in a position to give the weak form of the Maxwell model (1.1). By introducing the velocity variable $v = u_t$, the model changes into a velocity-stress form:

$$\begin{cases} \rho v_t = \mathbf{div} \sigma + f(x, t), & (x, t) \in \Omega \times [0, T], \\ \sigma + \sigma_t = \mathbb{C}\varepsilon(v), & (x, t) \in \Omega \times [0, T], \\ v = 0, & (x, t) \in \partial\Omega \times [0, T], \\ v(x, 0) = \phi_1(x), \sigma(x, 0) = \psi_0(x), & x \in \Omega. \end{cases} \quad (2.4)$$

Remark 2.1. Notice that $u(x, t) = \phi_0(x) + \int_0^t v(x, s) ds$.

Based on the Hellinger-Reissner variational principle, the weak problem for (1.1) reads as: Find $(\sigma, v) \in C^1([0, T], \underline{\mathbb{H}}(\mathbf{div}, \Omega, S)) \times C^1([0, T], \underline{L}^2(\Omega))$ such that

$$\begin{cases} a(\sigma_t, \tau) + a(\sigma, \tau) + b(v, \tau) = 0, & \forall \tau \in \underline{\mathbb{H}}(\mathbf{div}, \Omega, S), \\ c(v_t, w) - b(w, \sigma) = (f, w), & \forall w \in \underline{L}^2(\Omega), \\ v(x, 0) = \phi_1, \sigma(x, 0) = \psi_0. & \end{cases} \quad (2.5)$$

Here

$$a(\sigma, \tau) := \int_{\Omega} \mathbb{C}^{-1} \sigma : \tau dx, \quad b(v, \tau) := \int_{\Omega} v \cdot \mathbf{div} \tau dx, \quad c(v, w) := \int_{\Omega} \rho v \cdot w dx,$$

where $\tilde{\tau} : \tau = \sum_{i,j=1}^2 \tilde{\tau}_{ij} \tau_{ij}$ for $\tilde{\tau}, \tau \in \underline{\mathbb{H}}(\mathbf{div}, \Omega, S)$.

For any $\tau \in \underline{\mathbb{H}}(\mathbf{div}, \Omega, S)$, $w \in \underline{L}^2(\Omega)$, define

$$\|\tau\|_a^2 := a(\tau, \tau), \quad \|w\|_c^2 := c(w, w).$$

Then, according to (1.2) and (1.3), it holds

$$\sqrt{M_0} \|\tau\|_0 \leq \|\tau\|_a \leq \sqrt{M_1} \|\tau\|_0, \quad \sqrt{\rho_0} \|w\|_0 \leq \|w\|_c \leq \sqrt{\rho_1} \|w\|_0, \quad (2.6)$$

which also give

$$M_0 \|\tau\|_0^2 \leq a(\tau, \tau), \quad \rho_0 \|w\|_0^2 \leq c(w, w). \quad (2.7)$$

Simultaneously, the following stability conditions hold ([7]):

(i) Coercivity of $a(\cdot, \cdot)$ on $Z := \{\tau \in \underline{\mathbb{H}}(\mathbf{div}, \Omega, S); b(v, \tau) = 0, \forall v \in \underline{L}^2(\Omega)\}$:

$$\|\tau\|_{\mathbf{div}}^2 \lesssim a(\tau, \tau) \quad \forall \tau \in \underline{\mathbb{H}}(\mathbf{div}, \Omega, S),$$

where $\|\tau\|_{\mathbf{div}}^2 := \|\tau\|_0^2 + \|\mathbf{div}\tau\|_0^2$.

(ii) Inf-sup condition for $b(\cdot, \cdot)$:

$$\|w\|_0 \lesssim \sup_{0 \neq \tau \in \underline{\mathbb{H}}(\mathbf{div}, \Omega, S)} \frac{b(w, \tau)}{\|\tau\|_{\mathbf{div}}} \quad \forall w \in \underline{L}^2(\Omega).$$

From [22, Theorem 5.1], the following result of existence and uniqueness holds.

Lemma 2.1. *Suppose $\phi_0 \in \underline{H}_0^1(\Omega)$, $\phi_1 \in \underline{L}^2(\Omega)$, $\sigma_0 \in \underline{\mathbb{H}}(\mathbf{div}, \Omega, S)$ and $f \in C^0([0, T], \underline{L}^2(\Omega))$, then the weak problem (2.5) admits a unique solution $(\sigma, v) \in C^1([0, T], \underline{\mathbb{H}}(\mathbf{div}, \Omega, S)) \times C^1([0, T], \underline{L}^2(\Omega))$.*

3 Semi-discrete mixed finite element method

In this section, we discuss the semi-discrete finite element discretization of (2.5) and analyze its convergence under a general conforming mixed FEM framework.

3.1 Semi-discrete scheme

Assume that Ω is a convex polygonal domain, and let $\mathcal{T}_h = \bigcup\{T\}$ be a shape regular partition of Ω consisting of triangles or rectangles. For any $T \in \mathcal{T}_h$, let h_T denote its diameter, and we set $h := \max_{T \in \mathcal{T}_h} h_T$. For any integers $k, s \geq 0$, $P_k(T)$ denotes the set of all polynomials on T of degree at most k , and $P_{k,s}(T)$ the set of all polynomials of degree at most k in x and of degree at most s in y . Denote $Q_k(T) := P_{k,k}(T)$.

Let $\underline{\mathbb{H}}_h \subset \underline{\mathbb{H}}(\mathbf{div}, \Omega)$ and $\underline{V}_h \subset \underline{L}^2(\Omega)$ be two finite-dimensional spaces respectively for stress and velocity approximations on \mathcal{T}_h , satisfying the following condition:

(A1) Discrete inf-sup condition:

$$\|w_h\|_0 \lesssim \sup_{0 \neq \tau_h \in \underline{\mathbb{H}}_h} \frac{b(w_h, \tau_h)}{\|\tau_h\|_{\mathbf{div}}} \quad \forall w_h \in \underline{V}_h.$$

From (2.7) it directly follows

$$M_0 \|\tau_h\|_0^2 \leq a(\tau_h, \tau_h), \quad \rho_0 \|w_h\|_0^2 \leq c(w_h, w_h) \quad (3.1)$$

for any $\tau_h \in \underline{\mathbb{H}}_h, w_h \in \underline{V}_h$.

Let $\phi_{1,h}, \psi_{0,h}$ be respectively approximations of initial data ϕ_1 and ψ_0 , then the generic semi-discrete mixed conforming finite element scheme reads as: Find $(\sigma_h, v_h) \in C^1([0, T], \underline{\mathbb{H}}_h) \times C^1([0, T], \underline{V}_h)$ such that

$$\begin{cases} a(\sigma_{h,t}, \tau_h) + a(\sigma_h, \tau_h) + b(v_h, \tau_h) = 0, & \forall \tau_h \in \underline{\mathbb{H}}_h, \\ c(v_{h,t}, w_h) - b(w_h, \sigma_h) = (f, w_h), & \forall w_h \in \underline{V}_h, \\ v_h(x, 0) = \phi_{1,h}, \sigma_h(x, 0) = \psi_{0,h}. \end{cases} \quad (3.2)$$

By using standard techniques, we can obtain the following conclusion.

Lemma 3.1. *The semi-discrete scheme (3.2) admits a unique solution (σ_h, v_h) .*

Proof. Let $\{\varphi_i\}_{i=1}^r, \{\kappa_i\}_{i=1}^s$ be bases of $\underline{\underline{H}}_h$ and \underline{V}_h respectively. Let (i,j)-th components of matrix A, B, C be

$$(\mathbb{C}^{-1}\varphi_j, \varphi_i), (\mathbf{div}\varphi_j, \kappa_i), (\kappa_j, \kappa_i),$$

respectively. We write $\sigma_h = \sum_i \alpha_i \varphi_i, v_h = \sum_i \beta_i \kappa_i, \eta_j = (f, \kappa_j)$, and denote by α, β, η the corresponding vectors, respectively. Then we rewrite (3.2) as a matrix equation of the form

$$\begin{pmatrix} A & 0 \\ 0 & C \end{pmatrix} \begin{pmatrix} \alpha_t \\ \beta_t \end{pmatrix} = \begin{pmatrix} -A & -B \\ 0 & B^T \end{pmatrix} \begin{pmatrix} \alpha \\ \beta \end{pmatrix} + \begin{pmatrix} 0 \\ \eta \end{pmatrix} \quad (3.3)$$

The coefficient matrix on the left side of the equation is nonsingular because A, C are symmetric positive definite. Thus, due to the standard theory of ordinary differential equations, the system (3.3), and also (3.2), admits a unique solution. \blacksquare

3.2 Error estimation

To carry out the error estimation, we need to introduce, for the solution $(\sigma(t), v(t)) \in \underline{\underline{H}}(\mathbf{div}, \Omega, S) \times \underline{L}^2(\Omega)$ to the weak problem (2.5), an “elliptic projection” $(\Pi_1\sigma, \Pi_2v) \in \underline{\underline{H}}_h \times \underline{V}_h$ which are defined as follows: for $t \in [0, T]$, let $(\Pi_1\sigma, \Pi_2v) := (\hat{\sigma}_h(t), \hat{v}_h(t)) \in \underline{\underline{H}}_h \times \underline{V}_h$ satisfy

$$\begin{cases} a(\hat{\sigma}_h(t), \tau_h) + b(\hat{v}_h(t), \tau_h) = -a(\partial_t \sigma, \tau_h), & \forall \tau_h \in \underline{\underline{H}}_h, \\ b(w_h, \hat{\sigma}_h(t)) = b(w_h, \sigma) = c(v_t, w_h) - (f, w_h), & \forall w_h \in \underline{V}_h. \end{cases} \quad (3.4)$$

By (A1) and (3.1) it is easy to see that the “elliptic projection” is well-defined.

To derive convergence rates we also make the following regularity and approximation assumptions:

(A2) Let (σ, v) , the weak solution to (2.5), and its elliptic projection $(\hat{\sigma}_h(t), \hat{v}_h(t))$ satisfy the regularity conditions

$$\begin{cases} \sigma \in L^\infty([0, T], \underline{\underline{H}}^m(\Omega)), \quad \sigma_t \in L^2([0, T], \underline{\underline{H}}^m(\Omega)), \\ v \in L^\infty([0, T], \underline{H}^{m'}(\Omega)), \quad v_t \in L^2([0, T], \underline{H}^{m'}(\Omega)), \end{cases} \quad (3.5)$$

and the approximation conditions

$$\begin{cases} \|\hat{\sigma}_h - \sigma\|_0 + \|\hat{v}_h - v\|_0 \lesssim h^l(\|\sigma\|_m + \|v\|_{m'}), \\ \|\hat{\sigma}_{h,t} - \sigma_t\|_0 + \|\hat{v}_{h,t} - v_t\|_0 \lesssim h^l(\|\sigma_t\|_m + \|v_t\|_{m'}), \end{cases} \quad (3.6)$$

where $l, m, m' \geq 0$ are integers, and $g_{h,t} := \partial g_h / \partial t$ with $g = \hat{v}, \hat{\sigma}$.

Remark 3.1. *We note that the approximation estimates in (3.6) depend on the choice of $\underline{\underline{H}}_h$ and \underline{V}_h . Below are several examples which satisfy the discrete inf-sup condition (A1).*

- Arnold-Winther's triangular elements [2]:

$$\underline{\underline{\mathbf{H}}}_h = \left\{ \tau \in \underline{\underline{\mathbf{H}}}(\mathbf{div}, \Omega, S); \tau_{ij}|_T \in P_{k+2}(T), \mathbf{div}(\tau|_T) \in P_k(T)^2 \forall T \in \mathcal{T}_h \right\},$$

$$\underline{\mathbf{V}}_h = \left\{ w \in \underline{L}^2(\Omega); w|_T \in P_k(T) \forall T \in \mathcal{T}_h \right\},$$

where $k \geq 1$. The estimates in (3.6) hold with $l = m = k + 1$ and $m' = k + 2$.

- Arnold-Awanou's rectangular elements [1]:

$$\underline{\underline{\mathbf{H}}}_h = \left\{ \tau \in \underline{\underline{\mathbf{H}}}(\mathbf{div}, \Omega, S); \tau_{11}|_T \in P_{k+4,k+2}(T), \tau_{12}|_T \in P_{k+3,k+3}(T), \right.$$

$$\left. \tau_{22}|_T \in P_{k+2,k+4}(T) \forall T \in \mathcal{T}_h \right\},$$

$$\underline{\mathbf{V}}_h = \left\{ w \in \underline{L}^2(\Omega); w_1|_T \in P_{k+1,k}(T), w_2|_T \in P_{k,k+1}(T) \forall T \in \mathcal{T}_h \right\},$$

where $k \geq 1$. The estimates in (3.6) hold with $l = m = k + 1$ and $m' = k + 2$.

- Hu-Zhang's triangular elements [15, 17]:

$$\underline{\underline{\mathbf{H}}}_h = \left\{ \tau \in \underline{\underline{\mathbf{H}}}(\mathbf{div}, \Omega, S); \tau_{ij}|_T \in P_{k+1}(T) \forall T \in \mathcal{T}_h \right\},$$

$$\underline{\mathbf{V}}_h = \left\{ w \in \underline{L}^2(\Omega); w|_T \in P_k(T) \forall T \in \mathcal{T}_h \right\},$$

where $k \geq 2$. The estimates in (3.6) hold with $l = m' = k + 1$ and $m = k + 2$.

- Hu-Man-Zhang's rectangular element [16]:

$$\underline{\underline{\mathbf{H}}}_h = \left\{ \tau \in \underline{\underline{\mathbf{H}}}(\mathbf{div}, \Omega, S); \tau_{11} \in P_{2,0}(T), \tau_{22} \in P_{0,2}(T), \tau_{12} \in Q_1(T) \forall T \in \mathcal{T}_h \right\},$$

$$\underline{\mathbf{V}}_h = \left\{ w \in \underline{L}^2(\Omega); w_1 \in P_{1,0}(T), w_2 \in P_{0,1}(T) \forall T \in \mathcal{T}_h \right\}.$$

The estimates in (3.6) hold with $l = m' = 1$ and $m = 2$.

- Nedelec's rectangular elements [4, 23]:

$$\underline{\underline{\mathbf{H}}}_h = \left\{ \tau \in \underline{\underline{\mathbf{H}}}(\mathbf{div}, \Omega, S); \tau_{ij}|_T \in Q_{k+1}(T) \forall T \in \mathcal{T}_h \right\},$$

$$\underline{\mathbf{V}}_h = \left\{ w \in \underline{L}^2(\Omega); w_i|_T \in Q_k(T) \forall T \in \mathcal{T}_h \right\},$$

where $k \geq 0$. The estimates in (3.6) hold with $l = k + 1$ and $m = m' = k + 2$. We mention that in [4] the degrees of freedom of Nedelec's rectangular elements [23] $Q_{k+1}^{\mathbf{div}} - Q_k$ ($k \geq 0$) are modified so as to allow mass lumping.

In what follows, we choose the initial data in (3.2) as

$$\psi_{0,h} = I_{\mathbf{H}_h} \psi_0, \quad \phi_{1,h} = I_{\mathbf{V}_h} \phi_1, \quad (3.7)$$

where $I_{\mathbf{H}_h} : \underline{\underline{\mathbf{H}}}(\mathbf{div}, \Omega, S) \rightarrow \underline{\underline{\mathbf{H}}}_h$, $I_{\mathbf{V}_h} : \underline{L}^2(\Omega) \rightarrow \underline{\mathbf{V}}_h$ be two interpolation operators satisfying

$$\|\psi_0 - I_{\mathbf{H}_h} \psi_0\|_0 \lesssim h^l \|\psi_0\|_l, \quad \|\phi_1 - I_{\mathbf{V}_h} \phi_1\|_0 \lesssim h^l \|\phi_1\|_l \quad (3.8)$$

for $\psi_0 \in \underline{\underline{\mathbf{H}}}^l(\Omega)$, $\phi_1 \in \underline{\mathbf{H}}^l(\Omega)$.

Theorem 3.1. Let $(\sigma, v) \in C^1([0, T], \underline{\underline{\mathbf{H}}}(\mathbf{div}, \Omega, S)) \times C^1([0, T], \underline{\underline{L}}^2(\Omega))$ be the solution of the weak problem (2.5) and $(\sigma_h, v_h) \in C^1([0, T], \underline{\underline{\mathbf{H}}}_h) \times C^1([0, T], \underline{\underline{\mathbf{V}}}_h)$ be the solution of the semi-discrete problem (3.2). Then, under the assumptions (A1), (A2) and (3.8) we have

$$\begin{aligned} & \|\sigma - \sigma_h\|_{L^\infty([0, T], L^2)} + \|v - v_h\|_{L^\infty([0, T], L^2)} \\ & \lesssim h^l (\|\psi_0\|_l + \|\phi_1\|_l + \|\sigma\|_{L^\infty(H^m)} + \|\sigma_t\|_{L^2(H^m)} + \|v\|_{L^\infty(H^{m'})} + \|v_t\|_{L^2(H^{m'})}). \end{aligned} \quad (3.9)$$

Proof. In light of (3.6), (3.4) and the triangle inequality, it suffices to show the estimate

$$\|\hat{\sigma}_h - \sigma_h\|_0 + \|\hat{v}_h - v_h\|_0 \lesssim h^l (\|\psi_0\|_l + \|\phi_1\|_l + \|\sigma_t\|_{L^2(H^m)} + \|v_t\|_{L^2(H^{m'})}). \quad (3.10)$$

From (3.4) and (2.5) it follows

$$\begin{aligned} & a(\partial_t(\sigma - \sigma_h), \tau_h) + a(\hat{\sigma}_h - \sigma_h, \tau_h) + b(\hat{v}_h - v_h, \tau_h) = 0, \quad \forall \tau_h \in \underline{\underline{\mathbf{H}}}_h, \\ & c(\partial_t(v - v_h), w_h) = b(w_h, \hat{\sigma}_h - \sigma_h), \quad \forall w_h \in \underline{\underline{\mathbf{V}}}_h. \end{aligned}$$

Denote $\tilde{\sigma}_h := \hat{\sigma}_h - \sigma_h$, $\tilde{v}_h := \hat{v}_h - v_h$, and take $\tau_h = \tilde{\sigma}_h$, $w_h = \tilde{v}_h$ in the above two equations, then we get

$$a(\partial_t(\sigma - \sigma_h), \tilde{\sigma}_h) + a(\tilde{\sigma}_h, \tilde{\sigma}_h) + c(\partial_t(v - v_h), \tilde{v}_h) = 0,$$

which yields

$$a(\partial_t(\sigma - \sigma_h), \tilde{\sigma}_h) + c(\partial_t(v - v_h), \tilde{v}_h) \leq 0.$$

This, together with the relations $\sigma - \sigma_h = \sigma - \hat{\sigma}_h + \tilde{\sigma}_h$ and $v - v_h = v - \hat{v}_h + \tilde{v}_h$, implies

$$a(\partial_t \tilde{\sigma}_h, \tilde{\sigma}_h) + c(\partial_t \tilde{v}_h, \tilde{v}_h) \leq a(\partial_t(\hat{\sigma}_h - \sigma), \tilde{\sigma}_h) + c(\partial_t(\hat{v}_h - v), \tilde{v}_h),$$

Thus, by setting $E_h := a(\tilde{\sigma}_h, \tilde{\sigma}_h) + c(\tilde{v}_h, \tilde{v}_h)$ we can obtain

$$\begin{aligned} \frac{dE_h}{dt} & \leq 2a(\partial_t(\hat{\sigma}_h - \sigma), \tilde{\sigma}_h) + 2c(\partial_t(\hat{v}_h - v), \tilde{v}_h) \\ & \leq E_h + a(\partial_t(\hat{\sigma}_h - \sigma), \partial_t(\hat{\sigma}_h - \sigma)) + c(\partial_t(\hat{v}_h - v), \partial_t(\hat{v}_h - v)), \end{aligned}$$

where we have used the inequalities

$$2a(\sigma, \tau) \leq a(\sigma, \sigma) + a(\tau, \tau), \quad 2c(v, w) \leq c(v, v) + c(w, w).$$

By the continuous Gronwall inequality we deduce that

$$\begin{aligned} E_h & = \|\tilde{\sigma}_h\|_a^2 + \|\tilde{v}_h\|_c^2 \\ & \lesssim \|\tilde{\sigma}_h(0)\|_a^2 + \|\tilde{v}_h(0)\|_c^2 + \int_0^T \|\partial_t(\hat{\sigma}_h(s) - \sigma(s))\|_a^2 + \|\partial_t(\hat{v}_h(s) - v(s))\|_c^2 ds \end{aligned}$$

As a result, the desired estimate (3.10) follows from the initial data condition (3.8), the assumption (A2) and the equivalence of norms in (2.7). ■

4 Fully discrete mixed finite element method

4.1 Fully discrete scheme

Let $0 = t_0 < t_1 < \dots < t_M = T$ be a uniform division of time domain $[0, T]$, with $t_i = i\Delta t$ ($i = 0, 1, \dots, M$), and the time step size $\Delta t := \frac{T}{M}$. For any function $\varphi(t)$, we set

$$\varphi^n := \varphi(t_n), \quad \varphi^{n+\frac{1}{2}} := \frac{\varphi^n + \varphi^{n+1}}{2}, \quad \Delta_t \varphi^{n+\frac{1}{2}} := \frac{\varphi^{n+1} - \varphi^n}{\Delta t}.$$

Based on the semi-discrete scheme (3.2), a Crank-Nicolson full discretization scheme is given as follows: Find $(\sigma_h^{n+1}, v_h^{n+1}) \in \underline{\underline{H}_h} \times \underline{V}_h$ for $0 \leq n \leq M-1$ such that

$$\begin{cases} a(\Delta_t \sigma_h^{n+\frac{1}{2}}, \tau_h) + a(\sigma_h^{n+\frac{1}{2}}, \tau_h) + b(v_h^{n+\frac{1}{2}}, \tau_h) = 0, & \forall \tau_h \in \underline{\underline{H}_h}, \\ c(\Delta_t v_h^{n+\frac{1}{2}}, w_h) - b(w_h, \sigma_h^{n+\frac{1}{2}}) = (f^{n+\frac{1}{2}}, w_h), & \forall w_h \in \underline{V}_h, \end{cases} \quad (4.1)$$

with the initial data $v_h^0 = \phi_{1,h}$ and $\sigma_h^0 = \psi_{0,h}$ given by (3.7).

Lemma 4.1. *The fully discrete scheme (4.1) admits a unique solution $(\sigma_h^{n+1}, v_h^{n+1})$ for $n = 0, 1, \dots, M-1$.*

Proof. We only need to show that, when given (σ_h^n, v_h^n) , the linear system (4.1) admits a unique solution $(\sigma_h^{n+1}, v_h^{n+1})$. Since this is a square system, it suffices to show that the homogeneous system

$$\begin{cases} a(\sigma_h^{n+1}, \tau_h) + \frac{\Delta t}{2} a(\sigma_h^{n+1}, \tau_h) + \frac{\Delta t}{2} b(v_h^{n+1}, \tau_h) = 0 & \forall \tau_h \in \underline{\underline{H}_h}, \\ c(v_h^{n+1}, w_h) - \frac{\Delta t}{2} b(w_h, \sigma_h^{n+1}) = 0 & \forall w_h \in \underline{V}_h \end{cases}$$

yields the conclusion that

$$\sigma_h^{n+1} = 0, \quad v_h^{n+1} = 0. \quad (4.2)$$

In fact, taking $\tau_h = \sigma_h^{n+1}$ and $w_h = v_h$ in the above system leads to

$$(1 + \frac{\Delta t}{2}) a(\sigma_h^{n+1}, \sigma_h^{n+1}) + c(v_h^{n+1}, v_h^{n+1}) = 0,$$

then (4.2) follows. This completes the proof. ■

4.2 Stability analysis

Lemma 4.2. *For $J = 1, 2, \dots, M$, it holds*

$$\|\sigma_h^J\|_a^2 + \|v_h^J\|_c^2 \leq 2\Delta t \sum_{n=0}^{J-1} (f^{n+\frac{1}{2}}, v_h^{n+\frac{1}{2}}) + \|\sigma_h^0\|_a^2 + \|v_h^0\|_c^2. \quad (4.3)$$

Proof. Take $\tau_h = \sigma_h^{n+\frac{1}{2}}$ and $w_h = v_h^{n+\frac{1}{2}}$ in (4.1) and add up the two equations, we then get

$$a(\Delta_t \sigma_h^{n+\frac{1}{2}}, \sigma_h^{n+\frac{1}{2}}) + a(\sigma_h^{n+\frac{1}{2}}, \sigma_h^{n+\frac{1}{2}}) + c(\Delta_t v_h^{n+\frac{1}{2}}, v_h^{n+\frac{1}{2}}) = (f^{n+\frac{1}{2}}, v_h^{n+\frac{1}{2}}).$$

By the symmetry of \mathbb{C}^{-1} , we deduce that

$$\begin{aligned} a(\Delta_t \sigma_h^{n+\frac{1}{2}}, \sigma_h^{n+\frac{1}{2}}) &= (\mathbb{C}^{-1} \Delta_t \sigma_h^{n+\frac{1}{2}}, \sigma_h^{n+\frac{1}{2}}) = (\mathbb{C}^{-1} \frac{\sigma_h^{n+1} - \sigma_h^n}{\Delta t}, \frac{\sigma_h^{n+1} + \sigma_h^n}{2}) \\ &= \frac{1}{2\Delta t} (||\sigma_h^{n+1}||_a^2 - ||\sigma_h^n||_a^2). \end{aligned}$$

Similiarity, we have

$$c(\Delta_t v_h^{n+\frac{1}{2}}, v_h^{n+\frac{1}{2}}) = \frac{1}{2\Delta t} (||v_h^{n+1}||_c^2 - ||v_h^n||_c^2).$$

From the two relations above it follows that

$$\frac{1}{2\Delta t} (||\sigma_h^{n+1}||_a^2 - ||\sigma_h^n||_a^2 + ||v_h^{n+1}||_c^2 - ||v_h^n||_c^2) + ||\sigma_h^{n+\frac{1}{2}}||_a^2 = (f^{n+\frac{1}{2}}, v_h^{n+\frac{1}{2}}).$$

Summing up this equation from $n = 0, 1, \dots, J-1$ gives

$$||\sigma_h^J||_a^2 + ||v_h^J||_c^2 + 2\Delta t \sum_{n=0}^{J-1} ||\sigma_h^{n+\frac{1}{2}}||_a^2 = 2\Delta t \sum_{n=0}^{J-1} (f^{n+\frac{1}{2}}, v_h^{n+\frac{1}{2}}) + ||\sigma_h^0||_a^2 + ||v_h^0||_c^2,$$

which indicates the desired result. \blacksquare

Theorem 4.1. *Assume $\Delta t < 1$, then the full discretization scheme (4.1) is unconditionally stable in the following sense: For $J=1,2,\dots,M$, it holds*

$$||v_h^J||_c^2 + ||\sigma_h^J||_a^2 \lesssim \left(||\sigma_h^0||_a^2 + ||v_h^0||_c^2 + T \rho^{-1} \left(\max_{t \in [0,T]} ||f(t)||_0 \right)^2 \right) \times \exp(2T). \quad (4.4)$$

Proof. From (4.3) and Cauchy-Schwarz inequality we get

$$||\sigma_h^J||_a^2 + ||v_h^J||_c^2 \leq \Delta t \sum_{n=0}^{J-1} \rho^{-1} ||f^{n+\frac{1}{2}}||_V^2 + \Delta t \sum_{n=0}^{J-1} ||v_h^{n+\frac{1}{2}}||_c^2 + ||\sigma_h^0||_a^2 + ||v_h^0||_c^2.$$

On the other hand,

$$\begin{aligned} \sum_{n=0}^{J-1} ||v_h^{n+\frac{1}{2}}||_c^2 &= \sum_{n=0}^{J-1} \left| \left| \frac{v_h^{n+1} + v_h^n}{2} \right| \right|_c^2 \leq \frac{1}{2} \left(\sum_{n=0}^{J-1} ||v_h^{n+1}||_c^2 + \sum_{n=0}^{J-1} ||v_h^n||_c^2 \right) \\ &\leq \sum_{n=0}^{J-1} ||v_h^n||_c^2 + \frac{1}{2} ||v_h^J||_c^2. \end{aligned}$$

Since $\Delta t < 1$, the above two inequalities indicate

$$\frac{1}{2} ||v_h^J||_c^2 + ||\sigma_h^J||_a^2 \leq \Delta t \sum_{n=0}^{J-1} \rho^{-1} ||f^{n+\frac{1}{2}}||_V^2 + \Delta t \sum_{n=0}^{J-1} ||v_h^n||_c^2 + ||\sigma_h^0||_a^2 + ||v_h^0||_c^2,$$

which, together with the discrete Gronwall's inequality, yields (4.4). \blacksquare

4.3 Error estimation

Lemma 4.3. *Let (σ_h^j, v_h^j) ($j = 1, 2, \dots, M$) and $(\hat{\sigma}_h, \hat{v}_h)$ be respectively the solutions to the fully discrete scheme (4.1) and the semi-discrete "elliptic projection" problem (3.4), then it holds*

$$\begin{aligned} & \max_{1 \leq j \leq M} \|\sigma_h^j - \hat{\sigma}_h(t_j)\|_a + \max_{1 \leq j \leq M} \|v_h^j - \hat{v}_h(t_j)\|_c \\ & \lesssim \|\sigma_h^0 - \hat{\sigma}_h(0)\|_0 + \|v_h^0 - \hat{v}_h(0)\|_0 \\ & \quad + \Delta t \left(\sum_{j=0}^{M-1} \|\partial_t \sigma^{j+\frac{1}{2}} - \Delta_t \hat{\sigma}_h^{j+\frac{1}{2}}\|_0 + \sum_{j=0}^{M-1} \|\partial_t v^{j+\frac{1}{2}} - \Delta_t \hat{v}_h^{j+\frac{1}{2}}\|_0 \right). \end{aligned} \quad (4.5)$$

Proof. Setting $\psi_h^\alpha := \sigma_h^\alpha - \hat{\sigma}_h(t_\alpha)$, $r_h^\alpha := v_h^\alpha - \hat{v}_h(t_\alpha)$ for any index α and taking $t = t_j$, t_{j+1} in (3.4) respectively, from (4.1) we have, for $\forall \tau_h \in \underline{\mathbf{H}}_h$ and $w_h \in \underline{\mathbf{V}}_h$,

$$\begin{cases} a(\psi_h^{j+\frac{1}{2}}, \tau_h) + b(r_h^{j+\frac{1}{2}}, \tau_h) = -a(\Delta_t \psi_h^{j+\frac{1}{2}}, \tau_h) + a(\partial_t \sigma^{j+\frac{1}{2}} - \Delta_t \hat{\sigma}_h^{j+\frac{1}{2}}, \tau_h), \\ b(w_h, \psi_h^{j+\frac{1}{2}}) = c(\Delta_t r_h^{j+\frac{1}{2}}, w_h) + c(\Delta_t \hat{v}_h^{j+\frac{1}{2}} - \partial_t v^{j+\frac{1}{2}}, w_h). \end{cases}$$

Take $\tau_h = \psi_h^{j+\frac{1}{2}}$ and $w_h = r_h^{j+\frac{1}{2}}$ in these two equations, respectively, then we obtain

$$\begin{aligned} a(\psi_h^{j+\frac{1}{2}}, \psi_h^{j+\frac{1}{2}}) + b(r_h^{j+\frac{1}{2}}, \psi_h^{j+\frac{1}{2}}) &= -a(\Delta_t \psi_h^{j+\frac{1}{2}}, \psi_h^{j+\frac{1}{2}}) + a(\partial_t \sigma^{j+\frac{1}{2}} - \Delta_t \hat{\sigma}_h^{j+\frac{1}{2}}, \psi_h^{j+\frac{1}{2}}), \\ b(r_h^{j+\frac{1}{2}}, \psi_h^{j+\frac{1}{2}}) &= c(\Delta_t r_h^{j+\frac{1}{2}}, r_h^{j+\frac{1}{2}}) + c(\Delta_t \hat{v}_h^{j+\frac{1}{2}} - \partial_t v^{j+\frac{1}{2}}, r_h^{j+\frac{1}{2}}). \end{aligned}$$

Subtracting the second one of the above two equations from the first one, we arrive at

$$\begin{aligned} & a(\psi_h^{j+\frac{1}{2}}, \psi_h^{j+\frac{1}{2}}) + c(\Delta_t r_h^{j+\frac{1}{2}}, r_h^{j+\frac{1}{2}}) + a(\Delta_t \psi_h^{j+\frac{1}{2}}, \psi_h^{j+\frac{1}{2}}) \\ & = a(\partial_t \sigma^{j+\frac{1}{2}} - \Delta_t \hat{\sigma}_h^{j+\frac{1}{2}}, \psi_h^{j+\frac{1}{2}}) + c(\partial_t v^{j+\frac{1}{2}} - \Delta_t \hat{v}_h^{j+\frac{1}{2}}, r_h^{j+\frac{1}{2}}), \end{aligned}$$

which implies

$$\begin{aligned} & \frac{1}{2\Delta t} (\|\psi_h^{j+1}\|_a^2 - \|\psi_h^j\|_a^2 + \|r_h^{j+1}\|_c^2 - \|r_h^j\|_c^2) \\ & \lesssim a(\partial_t \sigma^{j+\frac{1}{2}} - \Delta_t \hat{\sigma}_h^{j+\frac{1}{2}}, \psi_h^{j+\frac{1}{2}}) + c(\partial_t v^{j+\frac{1}{2}} - \Delta_t \hat{v}_h^{j+\frac{1}{2}}, r_h^{j+\frac{1}{2}}), \end{aligned} \quad (4.6)$$

Multiplying this inequality by $2\Delta t$, and summing these equations for $j = 0, 1, \dots, j = n-1$ ($1 \leq n \leq M$), we get

$$\|\psi_h^n\|_a^2 + \|r_h^n\|_c^2 \lesssim \|\psi_h^0\|_a^2 + \|r_h^0\|_c^2 + A_1 + A_2, \quad (4.7)$$

with

$$\begin{aligned} A_1 &:= \Delta t \sum_{j=0}^{n-1} a(\partial_t \sigma^{j+\frac{1}{2}} - \Delta_t \hat{\sigma}_h^{j+\frac{1}{2}}, \psi_h^{j+1} + \psi_h^j), \\ A_2 &:= \Delta t \sum_{j=0}^{n-1} c(\partial_t v^{j+\frac{1}{2}} - \Delta_t \hat{v}_h^{j+\frac{1}{2}}, r_h^{j+1} + r_h^j). \end{aligned}$$

For the term A_1 , it holds

$$\begin{aligned}
A_1 &\leq \tilde{C} \Delta t \sum_{j=0}^{n-1} \|\partial_t \sigma^{j+\frac{1}{2}} - \Delta_t \hat{\sigma}_h^{j+\frac{1}{2}}\|_0 \|\psi_h^{j+1} + \psi_h^j\|_0 \\
&\leq 2\tilde{C} \Delta t \max_{0 \leq j \leq n} \|\psi_h^j\|_0 \left(\sum_{j=0}^{n-1} \|\partial_t \sigma^{j+\frac{1}{2}} - \Delta_t \hat{\sigma}_h^{j+\frac{1}{2}}\|_0 \right) \\
&\leq \frac{1}{2} \max_{0 \leq j \leq n} \|\psi_h^j\|_0^2 + 2(\tilde{C} \Delta t)^2 \left(\sum_{j=0}^{n-1} \|\partial_t \sigma^{j+\frac{1}{2}} - \Delta_t \hat{\sigma}_h^{j+\frac{1}{2}}\|_0 \right)^2,
\end{aligned} \tag{4.8}$$

where $\tilde{C} > 0$ is a constant depending on \mathbb{C}^{-1} and ρ . Similarly, we have

$$A_2 \leq \frac{1}{2} \max_{0 \leq j \leq n} \|r_h^j\|_0^2 + 2(\rho \Delta t)^2 \left(\sum_{j=0}^{n-1} \|\partial_t v^{j+\frac{1}{2}} - \Delta_t \hat{v}_h^{j+\frac{1}{2}}\|_0 \right)^2. \tag{4.9}$$

Putting (4.9) and (4.8) into (4.7) and noticing that $1 \leq n \leq M$, we finally get

$$\begin{aligned}
&\max_{1 \leq j \leq M} \|\psi_h^j\|_a^2 + \max_{1 \leq j \leq M} \|r_h^j\|_c^2 \\
&\lesssim \|\psi_h^0\|_0^2 + \|r_h^0\|_0^2 + (\Delta t)^2 \left(\sum_{j=0}^{M-1} \|\partial_t \sigma^{j+\frac{1}{2}} - \Delta_t \hat{\sigma}_h^{j+\frac{1}{2}}\|_0 \right)^2 \\
&\quad + (\Delta t)^2 \left(\sum_{j=0}^{M-1} \|\partial_t v^{j+\frac{1}{2}} - \Delta_t \hat{v}_h^{j+\frac{1}{2}}\|_0 \right)^2,
\end{aligned}$$

i.e. (4.5) holds true. ■

Lemma 4.4. *Under the assumption (A2) and the condition that*

$$\sigma_{tt} \in L^\infty([0, T], \underline{L}^2(\Omega)), \quad v_{tt} \in L^\infty([0, T], \underline{L}^2(\Omega)), \tag{4.10}$$

it holds, for $0 \leq j \leq M-1$,

$$\begin{aligned}
&\Delta t (\|\partial_t \sigma^{j+\frac{1}{2}} - \Delta_t \hat{\sigma}_h^{j+\frac{1}{2}}\|_0 + \|\partial_t v^{j+\frac{1}{2}} - \Delta_t \hat{v}_h^{j+\frac{1}{2}}\|_0) \\
&\lesssim h^l (\|\sigma\|_{L^\infty(H^m)} + \|v\|_{L^\infty(H^{m'})}) + (\Delta t)^2 (\|v_{tt}\|_{L^\infty(L^2)} + \|\sigma_{tt}\|_{L^\infty(L^2)}).
\end{aligned}$$

Proof. On one hand, using the Taylor expansion, we have

$$\partial_t \sigma^{j+\frac{1}{2}} - \Delta_t \sigma^{j+\frac{1}{2}} = \frac{1}{2} \int_{t_j}^{t_{j+1}} \sigma_{tt}(s) ds - \frac{1}{\Delta t} \int_{t_j}^{t_{j+1}} (t_{j+1} - s) \sigma_{tt}(s) ds,$$

which gives

$$\|\partial_t \sigma^{j+\frac{1}{2}} - \Delta_t \sigma^{j+\frac{1}{2}}\|_0 \lesssim \Delta t \|\sigma_{tt}\|_{L^\infty(L^2)}.$$

On the other hand, from (3.6) it follows

$$\begin{aligned}
\Delta t \|\Delta_t \sigma^{j+\frac{1}{2}} - \Delta_t \hat{\sigma}_h^{j+\frac{1}{2}}\|_0 &= \|\sigma(t_{j+1}) - \hat{\sigma}_h(t_{j+1}) - (\sigma(t_j) - \hat{\sigma}(t_j))\|_0 \\
&\lesssim h^l (\|\sigma\|_{L^\infty(H^m)} + \|v\|_{L^\infty(H^{m'})}).
\end{aligned}$$

As a result, by the triangle inequality we get

$$\Delta t \|\partial_t \sigma^{j+\frac{1}{2}} - \Delta_t \hat{\sigma}_h^{j+\frac{1}{2}}\|_0 \lesssim h^l (\|\sigma\|_{L^\infty(H^m)} + \|v\|_{L^\infty(H^{m'})}) + (\Delta t)^2 \|\sigma_{tt}\|_{L^\infty(L^2)}.$$

In the same way, we can obtain

$$\Delta t \|\partial_t v^{j+\frac{1}{2}} - \Delta_t \hat{v}_h^{j+\frac{1}{2}}\|_0 \lesssim h^l (\|\sigma\|_{L^\infty(H^m)} + \|v\|_{L^\infty(H^{m'})}) + (\Delta t)^2 \|v_{tt}\|_{L^\infty(L^2)}.$$

This finishes the proof. \blacksquare

Based on (3.6), (3.8), and Lemmas 4.3 and 4.4, it is easy to give the following error estimate for the fully discrete finite element scheme.

Theorem 4.2. *Let $(\sigma(t), v(t))$ be the solution to the weak problem (2.5) and (σ_h^n, v_h^n) ($n = 1, \dots, M$) be the solution to the fully discrete scheme (4.1) such that the assumptions (A1), (A2), (3.8) and (4.10) hold. Then it holds the error estimate*

$$\max_{1 \leq n \leq M} \|\sigma(t_n) - \sigma_h(t_n)\|_a + \max_{1 \leq n \leq M} \|v(t_n) - v_h(t_n)\|_c \lesssim C_1 h^l + C_2 (\Delta t)^2, \quad (4.11)$$

where $C_1 := \|\sigma\|_{L^\infty(H^m)} + \|v\|_{L^\infty(H^{m'})} + \|\psi_0\|_l + \|\phi_1\|_l$ and $C_2 := \|\sigma_{tt}\|_{L^\infty(L^2)} + \|v_{tt}\|_{L^\infty(L^2)}$.

Remark 4.1. *From Remark 3.1 and Theorem 4.2 we easily see that the error estimate (4.11) holds for*

- Arnold-Winther's triangular elements [2] and Arnold-Awanou's rectangular elements [1] with $l = m = k + 1$ ($k \geq 1$) and $m' = k + 2$;
- Hu-Zhang's triangular elements [15, 17] with $l = m' = k + 1$ ($k \geq 2$) and $m = k + 2$;
- Hu-Man-Zhang's rectangular element [16] with $l = m' = 1$ and $m = 2$;
- Nedelec's rectangular elements [4, 23] with $l = k + 1$ ($k \geq 0$) and $m = m' = k + 2$.

Remark 4.2. *Though only considering the Maxwell model (1.1) in two dimensions, we easily see that Theorems 3.1, 4.1 and 4.2 also hold for the three-dimensional case.*

5 Numerical results

As shown in Remark 4.1, there are many existing mixed conforming finite elements that can be used in the discretization of the Maxwell viscoelastic model (1.1). In our numerical examples, we shall apply two low order rectangular elements in the full discretization scheme (4.1).

- The lowest order modified Nedelec's rectangular element [4] ($k = 0$) with mass lumping: $Q_1^{\text{div}} - Q_0$ element. The corresponding finite-dimensional spaces are

$$\begin{aligned} \underline{\underline{\mathbf{H}}}_h &= \left\{ \tau \in \underline{\underline{\mathbf{H}}}(\mathbf{div}, \Omega, S); \tau_{ij}|_T \in Q_1(T) \ \forall T \in \mathcal{T}_h \right\}, \\ \underline{\mathbf{V}}_h &= \left\{ w \in \underline{\mathbf{L}}^2(\Omega); w_i|_T \in Q_0(T) \ \forall T \in \mathcal{T}_h \right\}, \end{aligned}$$

and the local degrees of freedom for the stress tensor $\sigma_h \in \underline{\underline{\mathbf{H}}}_h$ are $\sigma_h(x_i)$ ($i = 1, 2, 3, 4$), i.e. the values of σ_h at the four vertices, x_i , of rectangular element T . In the computation of $a(\cdot, \cdot)$, the following quadrature formula on T is used for mass lumping [4]:

$$\int_T g dx \approx \frac{h_x h_y}{4} \sum_{i=1}^4 g(x_i) \quad \forall g \in C^0(T),$$

where h_x and h_y are the side lengths of T .

- Hu-Man-Zhang's (abbr. HMZ) rectangular element [16]. We recall in this case that

$$\begin{aligned} \underline{\underline{\mathbf{H}}}_h &= \left\{ \tau \in \underline{\underline{\mathbf{H}}}(\mathbf{div}, \Omega, S); \tau_{11} \in P_{2,0}(T), \tau_{22} \in P_{0,2}(T), \tau_{12} \in Q_1(T) \ \forall T \in \mathcal{T}_h \right\}, \\ \underline{\mathbf{V}}_h &= \left\{ w \in \underline{L}^2(\Omega); w_1 \in P_{1,0}(T), w_2 \in P_{0,1}(T) \ \forall T \in \mathcal{T}_h \right\}. \end{aligned}$$

The local nodal degrees of freedom for the stress tensor are shown in Fig. 1.

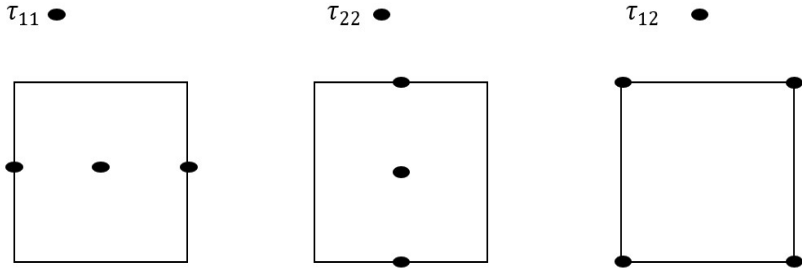


Figure 1: Nodal degrees of freedom for Hu-Man-Zhang's element

In the model problem (1.1), we take $\Omega = [0, 1] \times [0, 1]$, $T = 1$, and assume that the elastic medium is isotropic with $\rho = 1, \mu = 1, \lambda = 1$. We use $N \times N$ square meshes and M uniform grids for the spatial region Ω and the time region $[0, T]$. To test the accuracy, we compute the following errors for the stress and velocity approximations:

$$\begin{aligned} E_\sigma^a &= \max_{1 \leq n \leq M} \|\sigma(t_n) - \sigma_h(t_n)\|_a, \\ E_v^c &= \max_{1 \leq n \leq M} \|v(t_n) - v_h(t_n)\|_c. \end{aligned}$$

According to Theorem 4.2 and Remark 4.1, the theoretical accuracy of the full discretization is

$$E_\sigma^a + E_v^c \lesssim h + (\Delta t)^2 \approx N^{-1} + M^{-2}.$$

We consider the following three examples.

Example 5.1. The exact displacement field $u(x, y, t)$ and symmetric stress tensor $\sigma(x, y, t) = (\sigma_{ij})_{2 \times 2}$ are respectively given by

$$u = \begin{pmatrix} -e^{-t}(x^4 - 2x^3 + x^2)(4y^3 - 6y^2 + 2y) \\ -e^{-t}(y^4 - 2y^3 + y^2)(4x^3 - 6x^2 + 2x) \end{pmatrix},$$

$$\begin{pmatrix} \sigma_{11} \\ \sigma_{12} \\ \sigma_{22} \end{pmatrix} = \begin{pmatrix} 16te^{-t}(2x^3 - 3x^2 + x)(2y^3 - 3y^2 + y) \\ 2te^{-t}[(x^4 - 2x^3 + x^2)(6y^2 - 6y + 1) + (y^4 - 2y^3 + y^2)(6x^2 - 6x + 1)] \\ 16te^{-t}(2x^3 - 3x^2 + x)(2y^3 - 3y^2 + y) \end{pmatrix}.$$

Notice that the velocity field $v = u_t$. Numerical results of E_σ^a and E_v^a are shown in Tables 1 and 4.

Example 5.2. The exact displacement field u and symmetric stress tensor σ are respectively given by

$$u = \begin{pmatrix} -e^{-t}\sin(\pi x)\sin(\pi y) \\ -e^{-t}\sin(\pi x)\sin(\pi y) \end{pmatrix},$$

$$\begin{pmatrix} \sigma_{11} \\ \sigma_{12} \\ \sigma_{22} \end{pmatrix} = \begin{pmatrix} \pi te^{-t}(3\cos(\pi x)\sin(\pi y) + \sin(\pi x)\cos(\pi y)) \\ \pi te^{-t}(\sin(\pi x)\cos(\pi y) + \cos(\pi x)\sin(\pi y)) \\ \pi te^{-t}(3\sin(\pi x)\cos(\pi y) + \cos(\pi x)\sin(\pi y)) \end{pmatrix}.$$

Numerical results are shown in Tables 2 and 5.

Example 5.3. The exact displacement field u and symmetric stress tensor σ are respectively given by

$$u = \begin{pmatrix} e^t\sin(\pi x)(y^{3/2} - y^{5/2}) \\ e^t\sin(\pi y)(x^{3/2} - x^{5/2}) \end{pmatrix}, \quad (5.1)$$

$$\begin{pmatrix} \sigma_{11} \\ \sigma_{12} \\ \sigma_{22} \end{pmatrix} = \begin{pmatrix} \pi e^t(\frac{3}{2}\cos(\pi x)(y^{\frac{3}{2}} - y^{\frac{5}{2}}) + \frac{1}{2}\cos(\pi y)(x^{\frac{3}{2}} - x^{\frac{5}{2}})) \\ \frac{1}{2}e^t(\sin(\pi x)(\frac{3}{2}y^{\frac{1}{2}} - \frac{5}{2}y^{\frac{3}{2}}) + \sin(\pi y)(\frac{3}{2}x^{\frac{1}{2}} - \frac{5}{2}x^{\frac{3}{2}})) \\ \pi e^t(\frac{3}{2}\cos(\pi y)(x^{\frac{3}{2}} - x^{\frac{5}{2}}) + \frac{1}{2}\cos(\pi x)(y^{\frac{3}{2}} - y^{\frac{5}{2}})) \end{pmatrix}. \quad (5.2)$$

Numerical results are shown in Tables 3 and 6.

Tables 1, 2 and 3 give some numerical results at a fixed time step $\Delta t = 0.005$ to verify the theoretical first order spatial-accuracy of the schemes. Tables 4, 5 and 6 give numerical results with synchronous refinement of temporal and spatial meshes, $h = 4(\Delta t)^2$ or equivalently $N = M^2/4$, to verify the theoretical second order temporal-accuracy. From all the numerical results we have the following observations:

- As shown in Tables 1, 2 and 3, the HMZ element is of first order spatial accuracy, and the Nedelec's $Q_1^{\text{div}} - Q_0$ element gives better convergence rates than the first order for both E_σ^a and E_v^a .
- As shown in Tables 4, 5 and 6, the HMZ element is of second order temporal-accuracy, and the $Q_1^{\text{div}} - Q_0$ element yields higher than 2nd order convergence rates.
- For the $Q_1^{\text{div}} - Q_0$ element, the better convergence behaviours than the theoretical prediction may be due to some superconvergence of the element on square meshes.

Table 1: *Convergence history: Example 5.1 with $\Delta t = 0.005$.*

	$N \times N$	E_σ^a		E_v^c	
		error	order	error	order
$Q_1^{\text{div}} - Q_0$	4×4	0.0207	-	0.0066	-
	8×8	0.0111	0.89	0.0033	0.98
	16×16	0.0053	1.08	0.0016	1.08
	32×32	0.0019	1.49	0.0007	1.11
	64×64	0.0004	1.97	0.0003	1.22
HMZ	4×4	0.0097	-	0.0032	-
	8×8	0.0054	0.83	0.0018	0.86
	16×16	0.0028	0.96	0.0008	0.97
	32×32	0.0014	0.99	0.0004	0.99
	64×64	0.0007	1.00	0.0002	1.00

Table 2: *Convergence history: Example 5.2 with $\Delta t = 0.005$.*

	$N \times N$	E_σ^a		E_v^c	
		error	order	error	order
$Q_1^{\text{div}} - Q_0$	4×4	0.9423	-	0.4120	-
	8×8	0.5323	0.82	0.1925	1.10
	16×16	0.2245	1.25	0.0862	1.16
	32×32	0.0663	1.76	0.0355	1.28
	64×64	0.0157	2.08	0.0156	1.18
HMZ	4×4	0.3524	-	0.1587	-
	8×8	0.1784	0.98	0.0797	0.99
	16×16	0.0896	0.99	0.0399	1.00
	32×32	0.0448	1.00	0.0199	1.00
	64×64	0.0224	1.00	0.0100	1.00

Table 3: *Convergence history: Example 5.3 with $\Delta t = 0.005$.*

	$N \times N$	E_σ^a		E_v^c	
		error	order	error	order
$Q_1^{\text{div}} - Q_0$	4×4	0.6230	-	0.2136	-
	8×8	0.3480	0.84	0.1000	1.10
	16×16	0.1522	1.19	0.0422	1.25
	32×32	0.0460	1.73	0.0179	1.24
	64×64	0.0111	2.05	0.0081	1.14
HMZ	4×4	0.2531	-	0.0833	-
	8×8	0.1307	0.95	0.0425	0.97
	16×16	0.0661	0.98	0.0214	0.99
	32×32	0.0332	0.99	0.0107	1.00
	64×64	0.0167	1.00	0.0053	1.00

Table 4: *Convergence history: Example 5.1 with $N = M^2/4$.*

	M	E_σ^a		E_v^c	
		error	order	error	order
$Q_1^{\text{div}} - Q_0$	4	0.0096	-	0.0054	-
	8	0.0014	2.76	0.0013	2.02
	12	0.0004	2.91	0.0005	2.27
	16	0.0001	2.97	0.0002	2.22
HMZ	4	0.0097	-	0.0025	-
	8	0.0028	1.79	0.0007	1.66
	12	0.0013	1.98	0.0003	1.88
	16	0.0007	2.00	0.0002	1.93

Table 5: *Convergence history: Example 5.2 with $N = M^2/4$.*

	M	E_σ^a		E_v^c	
		error	order	error	order
$Q_1^{\text{div}} - Q_0$	4	0.3531	-	0.3231	-
	8	0.0404	3.13	0.0667	2.28
	12	0.0118	3.03	0.0268	2.24
	16	0.0049	3.05	0.0145	2.14
HMZ	4	0.3536	-	0.1253	-
	8	0.0896	1.98	0.0354	1.82
	12	0.0399	2.00	0.0164	1.90
	16	0.0224	2.00	0.0094	1.93

Table 6: *Convergence history: Example 5.3 with $N = M^2/4$.*

	M	E_σ^a		E_v^c	
		error	order	error	order
$Q_1^{\text{div}} - Q_0$	4	0.2601	-	0.2126	-
	8	0.0362	2.85	0.0396	2.42
	12	0.0117	2.78	0.0153	2.34
	16	0.0055	2.60	0.0081	2.21
HMZ	4	0.2528	-	0.0837	-
	8	0.0661	1.94	0.0215	1.96
	12	0.0295	1.99	0.0096	2.00
	16	0.0166	1.99	0.0054	2.00

References

- [1] D. N. Arnold and G. Awanou. Rectangular mixed finite elements for elasticity. *Mathematical Models and Methods in Applied Sciences*, 15(9):1417–1429, 2005.
- [2] D. N. Arnold and R. Winther. Mixed finite elements for elasticity. *Numerische Mathematik*, 92(3):401–419, 2002.

- [3] E. Becache, A. Ezziani, and P. Joly. A mixed finite element approach for viscoelastic wave propagation. *Computational Geosciences*, 8(3):255–299, 2005.
- [4] E. Becache, P. Joly, and C. Tsogka. A new family of mixed finite elements for the linear elastodynamic problem. *Siam Journal on Numerical Analysis*, 39(6):2109–2132, 2001.
- [5] D. R. Bland. The theory of linear viscoelasticity. Pergamon Press, 1960.
- [6] T. Bohlen. Parallel 3-d viscoelastic finite difference seismic modelling. *Computers & Geosciences*, 28(8):887–899, 2002.
- [7] F. Brezzi and M. Fortin. Mixed and hybrid finite element methods. Springer-Verlag, 1991.
- [8] R. M. Christensen. Theory of Viscoelasticity, An Introduction. Academic Press, 1982.
- [9] E.H. Dill. Continuum Mechanics : Elasticity, Plasticity, Viscoelasticity. CRC Press, 2007.
- [10] A. D. Drozdov. Mechanics of Viscoelastic Solids. Wiley, 1998.
- [11] Y. C Fung. International series on dynamics. (book reviews: Foundations of solid mechanics). *Science*, 152, 1966.
- [12] J. M. Golden and G. A. C. Graham. Boundary Value Problems in Linear Viscoelasticity. Springer, 1988.
- [13] M. E. Gurtin and E. Sternberg. On the linear theory of viscoelasticity. *Archive for Rational Mechanics and Analysis*, 11(1):291–356, 1962.
- [14] T. Ha, J.E. Santos, and D. Sheen. Nonconforming finite element methods for the simulation of waves in viscoelastic solids. *Computer Methods in Applied Mechanics & Engineering*, 191:5647–5670, 2002.
- [15] J. Hu. Finite element approximations of symmetric tensors on simplicial grids in r^n : the high order case. *Journal of Computational Mathematics*, 33(3):283–296, 2015.
- [16] J. Hu, H. Y. Man, and Zhang S. A simple conforming mixed finite element for linear elasticity on rectangular grids in any space dimension. *J Sci Comput*, 58:367–379, 2014.
- [17] J. Hu and S. Y. Zhang. A family of conforming mixed finite elements for linear elasticity on triangular grids. *arXiv:1406.7457*, 2014.
- [18] V. Janovsky, S. Shaw, M. K. Warby, and J. R. Whiteman. Numerical methods for treating problems of viscoelastic isotropic solid deformation. *Journal of Computational & Applied Mathematics*, 63(1-3):91–107, 1995.
- [19] M. Kimura, Notsu H., Y. Tanaka, and H. Yamamoto. The gradient flow structure of an extended maxwell viscoelastic model and a structure-preserving finite element scheme. *Journal of Scientific Computing*, 2018.

- [20] D. Kosloff, J.M. Carcione, and R. Kosloff. Wave propagation simulation in a linear viscoelastic medium. *Geophysical Journal*, 93:393–407, 1988.
- [21] D. Kosloff, J.M. Carcione, and R. Kosloff. Wave propagation simulation in a visco-elastic medium. *Geophysical Journal*, 95:597–611, 1988.
- [22] J. Lee. Mixed methods with weak symmetry for time dependent problems of elasticity and viscoelasticity. PhD thesis, University of Minnesota., 2012.
- [23] J. C. Nedelec. A new family of mixed finite elements in \mathcal{R}^3 . *Numerische Mathematik*, 50(1):57–81, 1986.
- [24] B. Riviere and S. Shaw. Discontinuous galerkin finite element approximation of nonlinear non-fickian diffusion in viscoelastic polymers. *Siam Journal on Numerical Analysis*, 44(6):2650–2670, 2006.
- [25] B. Riviere, S. Shaw, M. F. Wheeler, and J. R. Whiteman. Discontinuous galerkin finite element methods for linear elasticity and quasistatic linear viscoelasticity. *Numerische Mathematik*, 95(2):347–376, 2003.
- [26] B. Riviere, S. Shaw, and J. R. Whiteman. Discontinuous galerkin finite element methods for dynamic linear solid viscoelasticity problems. *Numerical Methods for Partial Differential Equations*, 23(5):1149–1166, 2007.
- [27] M.E. Rognes and R. Winther. Mixed finite element methods for linear viscoelasticity using weak symmetry. *Mathematical Models and Methods in Applied Sciences*, 20(06):955–985, 2010.
- [28] V. Sabinin, T. Chichinina, and G.R. Jarillo. *Numerical Model of Seismic Wave Propagation in Viscoelastic Media*. Springer Berlin Heidelberg, 2003.
- [29] J. Salencon. *Viscoélasticité pour le calcul des structures*. 2016.
- [30] R. A Schapery. Nonlinear viscoelastic solids. *International Journal of Solids and Structures*, 37(1–2):359–366, 2000.
- [31] P. C. M. Severino and J. C. Guillermo. *Computational Viscoelasticity*. Springer New York, 2012.
- [32] V. Thomee. Galerkin finite element methods for parabolic problems. *Mathematics of Computation*, 17(2):186–187, 2006.
- [33] S. Wang and X. Xie. Semi-discrete and fully discrete hybrid stress finite element methods for maxwell viscoelastic model of wave propagation. *Numerical Mathematics A Journal of Chinese Universities*, 42(3), 2020.
- [34] T. Xu and G.A. McMechan. Efficient 3-d viscoelastic modeling with application to near-surface land seismic data. *Geophysics*, 63(2):601–612, 1998.